Renewable Energy 218 (2023) 119242

Contents lists available at ScienceDirect

Renewable Energy

journal homepage: www.elsevier.com/locate/renene

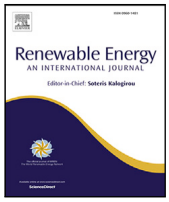

On the influence of mooring systems in optimal predictive control for wave energy converters

Guglielmo Papini *, Bruno Paduano, Edoardo Pasta, Fabio Carapellese, Giuliana Mattiazzo, Nicolás Faedo

Marine Offshore Renewable Energy Lab, Department of Mechanical and Aerospace Engineering, Politecnico di Torino, Via Duca degli Abruzzi, Turin, 10129, Piedmont, Italy

ARTICLE INFO

Keywords:
Wave energy
Model predictive control
Mooring system
Wave estimation
Wave prediction
System identification

ABSTRACT

Wave energy conversion systems have a massive potential in securing a reliable renewable energy mix. In their development, a crucial role is that of optimal control (OC) algorithms. Such systems are able to maximize the wave energy converter (WEC) power extraction, while respecting the corresponding of technological constraints. State-of-the-art OC techniques, such as Model Predictive Control (MPC), rely on mathematical models of the device to control, in a predictive fashion, the WEC system, thus maximizing the power production. Nonetheless, to date, control algorithms are usually developed and assessed on the basis of free floating WEC models, *i.e.* which neglect the mooring system influence. As a matter of fact, the anchorage introduces nonlinear dynamics in the device motion. Consequently, to test the idealized potential of a control strategy, such system is commonly neglected. Moorings are a fundamental WEC component, and have the potential to influence significantly the associated system dynamics. Neglecting this element can lead to deceptive results, either in terms of device theoretical productivity, and control strategy effectiveness. This paper proposes a systematic procedure to include, in the model used to synthesized such OC strategies, a linear representative model of the mooring system, presenting its benefits by discussing the consequent MPC loop development and corresponding performance assessment. Such procedure consists in retrieving an estimate of the frequency response of the moored system, using properly designed input conditions, and identifying the associated input–output linear system. A main objective of this study is, hence, to assess the difference between an MPC strategy designed and synthesized, with and without the proposed mooring control-oriented representation, always using as simulation system a high-fidelity numerical model for performance evaluation, which incorporates a full account of the mooring effects.

1. Introduction

Given the current worldwide emission situation, research is pushing its efforts towards finding alternative, CO_2 clean energy sources. Since renewable energies (such as solar, wave, and wind, among others), can be an interesting alternative compared to traditional, carbon-based power production systems, their harvesting technologies are under constant investigation and improvement. Among them, wave energy is a promising field, due to the continuous availability of its primary energy source and the considerable wave power potential [1].

Nevertheless, in contrast with wind and solar technologies, wave energy has not yet achieved economic viability, and research is pushing towards different alternatives to achieve commercialization stage [2]. One of the main open points regards the convergence to a standard device to reduce the associated production costs [3]. The devices in charge of extracting power from wave motion, called wave energy converters (WECs), are commonly composed of a floating body (hull) anchored to the seabed by means of an mooring system. The waves activate the hull motion and an electro-mechanical device, called power take-off (PTO) system, converts the mechanical energy into electrical, to then be injected into the grid.

Nonetheless, independently from the specific device nature, a crucial aspect in wave energy conversion regards the implementation of optimal control strategies, in charge of maximizing the device energy extraction from the wave resource, while respecting physical constraints to avoid system damage [4]. In this context, model-based control techniques constitute one of the most promising alternatives

* Corresponding author.
E-mail addresses: guglielmo.papini@polito.it (G. Papini), bruno.paduano@polito.it (B. Paduano), edoardo.pasta@polito.it (E. Pasta), fabio.carapellese@polito.it (F. Carapellese), giuliana.mattiazzo@polito.it (G. Mattiazzo), nicolas.faedo@polito.it (N. Faedo).

https://doi.org/10.1016/j.renene.2023.119242
Received 17 February 2023; Received in revised form 23 August 2023; Accepted 28 August 2023
Available online 31 August 2023

[5–8]. Such algorithms use a WEC model to compute the optimal theoretical motion/control law in a predictive fashion. Nevertheless, a main issue in computing such an optimal controller regards the non-causal nature of the optimization problem [9]. Since the optimality of the solution heavily depends on future wave excitation force values, which are not known in advance, suitable forecasting strategies must be employed to restore the underlying problem causality [10]. Additionally, to compensate the inability of physical sensors (*i.e.* hull pressure probes) to measure wave force in a moving object, auxiliary state observers are required to estimate such a signal [11].

Since the vast majority of WEC systems are located at a certain distance from shore [12], a vital component (previously mentioned within this section), which guarantees the proper functioning of such devices, is the mooring system, which is responsible of solving the station-keeping problem. Although the mooring system is generally analyzed only within so-called survivability conditions [13], its influence and relevance should not be considered only with respect to its withstanding (and survivability) features [14–16], but also in relation to the device operating conditions and, therefore, included within control design procedures. Given that optimal WEC control design involves the adoption of a suitable model able to effectively describe the device dynamics in a control-oriented fashion, if such a model does not represent consistently the WEC behavior, the optimality of the associated computed control solution can be compromised. The vast majority of design/assessment results presented within state-of-the-art WEC control strategies is carried out under the assumption, both in control-oriented modeling and in simulation (performance evaluation) stage, of negligible mooring effects [6,7]. This assumption, ostensibly adopted given the inherent complexity behind mooring models [17], can be significantly restrictive, since the mooring system can influence heavily the associated system dynamics and, consequently, any productivity analysis may return misleading power production results [14].

In the light of these considerations, this paper proposes a data-based modeling procedure for moored WEC systems, leveraging input/output data from a high-fidelity mooring solver. In particular, the latter is based upon the well-established solver OrcaFlex (OF) [18], where a moored heaving point absorber is considered (see Section 2.1 for further detail). Based on the model computed following the proposed methodology, which is first validated against the high-fidelity solver accordingly, a detailed account of the design and synthesis of an energy-maximizing model predictive controller (MPC) is presented, and effectively applied within the OF WEC solver. We show that the proposed data-based modeling methodology is able to capture the mooring dynamics in such a way that the control solution is effectively informed of the dynamics introduced by the anchorage in the overall system response, providing a convenient solution for the design and synthesis of realistic WEC MPC. Given the inherent non-causality of the WEC problem (see the discussion provided within this section), we design a corresponding wave excitation estimator and forecaster, to provide instantaneous and future values of the wave input, respectively. To further emphasize the importance of incorporating representative WEC models within effective control, aware of the inherent mooring dynamics, we present a detailed analysis on the influence of mooring systems in final performance assessment. To achieve this, we design a controller following the methodology employed by the vast majority of the state-of-the-art WEC control studies, *i.e.* we synthesize a MPC law using a model which does not provide a representative account of the underlying mooring dynamics, providing a comparison with the procedure proposed within this paper.

In summary, the main contributions of this study are as follows:

- To provide a simple methodology for data-based control-oriented modeling for moored WEC systems, able to incorporate the mooring dynamics swiftly.
- Validate this methodology against the numerical high-fidelity environment, *i.e.* against the full nonlinear moored WEC model.
- Synthesize a MPC strategy based on the proposed methodology and assess and compare its performance, employing, as control-oriented model, both that stemming from the proposed data-based approach, and that pursued by the state-of-the-art (*i.e.* models which does not incorporate an account of mooring effects within the WEC response operator).

The remainder of this paper is structured as follows. Section 1.1 provides an account of the main notation used throughout this paper. Section 2 describes the WEC heaving point absorber considered, and the main modeling preliminaries employed within the WEC field. Section 3 presents the proposed data-based modeling approach for moored WEC systems, while Section 4 provides a full account of the MPC loop, including optimization, and wave estimation and prediction algorithms. Finally, Section 5 details and discusses the obtained results while, in Section 6, the main conclusions of this study are encompassed.

1.1. Notation

Standard notation is used throughout this paper, with any exceptions listed within this section. The set of non-negative real numbers is denoted as $\mathbb{R}^+$. Given a function f, its Laplace transform (provided it exists) is denoted with capital letters, *i.e.* as $F(s)$, $s \in \mathbb{C}$. With some abuse of notation, its associated Fourier transform is simply denoted in terms of the restriction of $F(s)$ to $s \equiv j\omega$, *i.e.* $F(j\omega)$, $\omega \in \mathbb{R}$. Given a matrix $A \in \mathbb{C}^{n\times m}$ its transpose is denoted as $A^\mathsf{T} \in \mathbb{C}^{m\times n}$. The notation $\mathbb{N}_y$ is reserved for the set of natural numbers up to y, *i.e.* $\mathbb{N}_y = \{1, 2, \dots, y\} \subset \mathbb{N}$. Without exceptions, the dependence on the variable t is used to denote a continuous-time signal/system, *e.g.* a continuous signal $f(t)$, while the letter k is reserved for discrete-time elements, *e.g.* a sampled signal $f(k)$. The symbol $\mathbf{1}_n \in \mathbb{R}^n$ denotes a column-vector with all its entries equal to one. The notation $\mathbb{I}_n$ is used for the identity element of the space $\mathbb{C}^{n\times n}$. Finally, given a one-dimensional discrete-time signal $d(k)$, its 'projection' $D_i^j \in \mathbb{R}^{j-i}$ from sample i until j is defined as

$$D_i^j = \begin{bmatrix} d(k+i) & d(k+i+1) & \cdots & d(k+i+j) \end{bmatrix}^\mathsf{T}. \tag{1}$$

2. Device setup and modeling preliminaries

This section presents the case study adopted within this study, and summarizes the primary strategies employed in linear, control-oriented, modeling of wave energy extraction systems. The reader can refer to [19,20] for further detail regarding the assumptions considered in linear WEC modeling.

2.1. Device setup

The device considered for this study is a spherical heaving point absorber WEC, schematically represented in Fig. 1. Such a system comprises a floating sphere in which the vertical axis, z, is the energy extraction degree of freedom (DoF). Therefore, the vertical motion along the z-axis is responsible for energy extraction.

The point absorber is a spherical floating unit with the center of gravity located in the geometric center and, according to the free-floating condition, on the waterline (often referred to as still water level (SWL)). The chosen benchmark WEC system is hence designed considering a well-studied concept, featuring an ideal PTO, consistent with the literature in optimal WEC control (see [21]). In particular, the designed control action is directly applied on the vertical axis of the sphere, with mechanical energy conversion being the primary control objective (see Section 4.1). The mooring system is formed by a symmetrical pattern of four semi-taut mooring lines. The bottom catenary sections are used to prevent the synthetic section damage by avoiding the clash of the latter with the seabed, while the upper one avoids the synthetic line to work in the splash zone, which can be harmful for a synthetic-made line. Sub-surfaces buoys are adopted to ensure the proper working of the line (see Fig. 1). The main properties

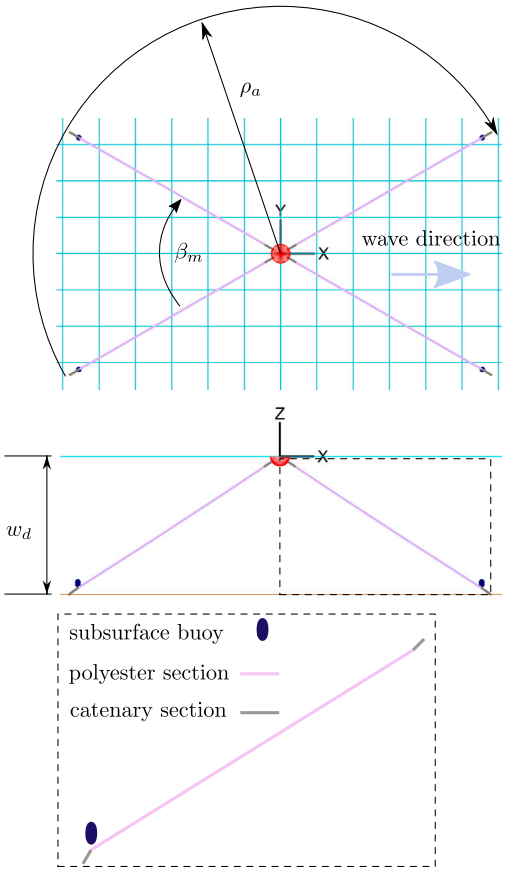

Fig. 1. OF representation of the point absorber. Global axes expressed according to the OF global frame of reference.

of the system are summarized in Table 1. Given the nature of the system under investigation, *i.e.* a heaving device, the properties are expressed with respect to the system response on heave. In addition, the main features of the solver are given in Table 1.

2.2. Modeling preliminaries: Time-domain equations

Following Newton's second law, the dynamic equation of the point absorber vertical displacement $z(t)$ can be written as:

$$m\ddot{z}(t) = f_h(t) + f_r(t) + f_w(t) + f_m(t) + u(t). \tag{2}$$

In Eq. (2), $t \in \mathbb{R}$ is the time, $m \in \mathbb{R}^+$ represents the mass of the device, $f_h : \mathbb{R}^+ \to \mathbb{R}$ is the hydrostatic force exerted on the hull, $f_r : \mathbb{R}^+ \to \mathbb{R}$ stands for radiation effects, $f_w : \mathbb{R}^+ \to \mathbb{R}$ indicates the wave excitation force effect imposed by the incoming wave field, $f_m : \mathbb{R}^+ \to \mathbb{R}$ is the mooring force acting on the hull, and $u : \mathbb{R}^+ \to \mathbb{R}$ is the control force applied by the PTO.

Within linear conditions, the radiation force f_r can be modeled as a convolution term via the so-called Cummins' equation [22], *i.e.*

$$f_r(t) = -m_\infty \ddot{z}(t) - \int_{\mathbb{R}} k_r(\tau)\dot{z}(t-\tau)d\tau, \tag{3}$$

where $m_\infty \in \mathbb{R}^+$ is the added mass at infinite frequency [23], the term $k_r(t) \in \mathbb{R}$ is the radiation force impulse response function. To solve Cummins' equation, the integral term is virtually always characterized, in a non-parametric form, via Boundary Elements Method (BEM) software, such as *e.g.* OrcaWave [18].

Remark 1. A critical aspect of any BEM software is that it provides a finite set of datapoints (either in the time- or frequency-domain) characterizing k_r, and not an analytical (*i.e.* closed-form) description for Eq. (3). As it is more accurately described in Section 2.3, the non-parametric nature of k_r leads to the consideration that system identification routines are required to effectively compute a parametric WEC model.

Table 1
Orcaflex solver main parameters (see [24] for further detail).

Property	Symbol	Value
Device		
Sphere radius	–	4 [m]
Mass	m	137 120 [kg]
Hydrostatic stiffness	k_h	504 000 [N/m]
Water depth	w_d	55 [m]
Water density	ρ_w	1025 kg/m^3
Mooring		
Anchor radius	ρ_a	100 [m]
Mooring angle	β_m	$\frac{\pi}{3}$ [rad]
Catenary s. length	–	5 [m]
Catenary size	–	0.05 [m]
Catenary elasticity modulus	–	252 000 [kN]
Catenary weight per [m] (off-water)	–	54.5 [kg/m]
Polyester s. length	–	100 [m]
Polyester diameter	–	0.1 [m]
Polyester elasticity modulus	–	10 000 [kN]
Polyester density	–	8.5 [kg/m^3]
Buoy NB	–	1000 [kg]

Continuing with the description of the forces in (2), the hydrostatic restoring force f_h can be modeled as a linear term

$$f_h(t) = -k_h z(t), \tag{4}$$

where $k_h \in \mathbb{R}^+$ is the hydrostatic restoring coefficient.

Finally, as previously discussed within Section 1, there is an intrinsic difficulty in deriving closed-form analytical expressions for the mooring force f_m compatible with control/estimation applications, *i.e.* which can provide a parsimonious balance between analytical/computational complexity and mooring model fidelity [17]. Furthermore, the nature of f_m intrinsically depends on the specific mooring configuration, hence complicating the issue of finding a generalized (tractable) expression for mooring dynamics.

Remark 2. We note that, as previously pointed out in the WEC control literature (see [25]), the inclusion of nonlinear hydrodynamic effects can also be effectively relevant for devices under controlled conditions. Nonetheless, the study presented within this paper is focused on the effect of mooring dynamics in the overall controller performance, which is completely disregarded in virtually all of WEC control literature available [21]. To that end, and in an effort to distinguish, *i.e.* isolate to the maximum extent possible, the effect of mooring systems in control synthesis and assessment from other potential sources of nonlinearity (such as those studied in [25]), linear potential flow conditions have been considered for simulation purposes, consistent with the vast majority of the optimal control related literature [21]. We note, however, that the data-based approach proposed within this paper can be effectively used in a more complex hydrodynamic scenario, by adjusting the high-fidelity model, which effectively produces the data for identification, accordingly.

2.3. Modeling preliminaries: Frequency-domain analysis

As discussed explicitly within Remark 1, BEM software are vastly employed to characterize WECs motion frequency response [23]. The vast majority of available BEM software operates in the frequency-domain, *i.e.* these provide a steady-state description of the device dynamics (in particular, a set of datapoints characterizing k_r in (3)) in a

finite set of frequency points, often specified as a user-defined input to the software. As such, we provide, in this section, a frequency-domain analysis of Eq. (2), which is later explicitly used for control-oriented modeling purposes.

Throughout this section, and as virtually always adopted within the WEC literature (see the discussion provided in Section 1), we assume that $f_m = 0$, $\forall t$. It is hence possible to link the Fourier transform of the vertical (heave) velocity $\dot{z} = v$ and the Fourier transform of the total input force $\xi = f_e + u$, in terms of a complex mapping $H_0 : \mathbb{C} \to \mathbb{C}$,

$$V(j\omega) = H_0(j\omega)\Xi(j\omega). \tag{5}$$

In particular, the map $H(j\omega)$ can be written in terms of a direct application of the Fourier transform to (2):

$$H_0(j\omega) = \left(K_r(j\omega) + j\omega\mathcal{M} + \frac{k_h}{j\omega} \right)^{-1}. \tag{6}$$

Given that an analytical form for $K_r(j\omega)$ is not available (see Remark 1), classical system identification techniques [26] are commonly used to compute a linear time-invariant (LTI) model from the frequency-response map $H_0(j\omega)$ in Eq. (6). This map, nonetheless, does not take into account an internal representation of the mooring effects, but simply those related to the hydrodynamic behavior of the WEC system. Leveraging the frequency-domain representation in (6), we propose, within Section 3, a data-based modeling procedure for WEC devices including mooring dynamics, which is compatible with optimal control procedures (as explicitly demonstrated within Section 4).

3. Data-based modeling of moored WEC systems

As discussed within Section 2.1, the device under investigation is station-kept by means of a symmetrical, spread, semi-taut mooring system. The high-fidelity model, also adopted as control target (simulation) system, is built in OF [24]. The software computes the interaction between a floating body and its mooring system, by numerically solving the convolution integral of the impulse response function in (3).

Within this section, and aiming to explicitly include the mooring influence within the overall WEC dynamics, we propose a data-based approach for control-oriented modeling of WEC moored systems. In particular, an input/output (I/O) identification approach is pursued, where a set of sufficiently exciting (see *e.g.* [27]) inputs is applied within the high-fidelity benchmark model in OF, and used to collect representative output data of the WEC device, comprising the corresponding influence of the mooring system.

Given that the wave excitation force f_w acting on heave 'shares' the same input channel as the mooring force (see Eq. (2), we define a set of I/O pairs (f_{w_j}, v_j), $j \in \mathbb{N}_{N_j}$, where each f_{w_j} denotes a so-called multisine signal

$$f_{w_j}(t) = \sum_{i=1}^{N_i} \gamma_j \cos(\omega_i t + \phi_i), \quad \phi_i = \frac{-i(i+1)}{N_i}, \tag{7}$$

i.e. each f_{w_j} is represented in terms of a periodic function with $N_i \in \mathbb{N}$ harmonics of a fundamental frequency $\omega_i \in \mathbb{R}$, $\forall i \in \mathbb{N}_{N_i}$, and an associated input amplitude $\gamma_j \in \mathbb{R}$. The particular expression used within (7) to describe the set of phases $\{\phi_i\}$ stems directly from the so-called Schroeder phases (see *e.g.* [28]).

Remark 3. Note that this type of signal can excite a specific frequency band, with a user-defined spectrum (*e.g.* flat, as in the case of (7) - see also Fig. 3), keeping an almost constant instantaneous amplitude in time, by virtue of a suitable selection of the set of phases. We further clarify that the limits associated with the exciting frequency band are intrinsically linked to the nature (*i.e.* dynamics), and operating conditions, of the moored WEC system to be approximated.

Having computed each associated I/O pair (with f_{w_j} as in (7)), the so-called empirical transfer function estimate (ETFE) $H_j(j\omega)$ can be computed for each (f_{w_j}, v_j), *i.e.*

$$H_j(j\omega) = \frac{V_j(j\omega)}{F_{w_j}(j\omega)}, \tag{8}$$

hence directly providing an estimate of the frequency response associated with the moored WEC system, by explicit use of the data generated within the corresponding high-fidelity OF model. In order to compute a *representative* control-oriented model, the set of amplitudes $\{\gamma_j\}_{j=1}^{N_j}$ is chosen so as to excite the system in its full operating range, guaranteeing a complete description of the device dynamics before effective parameterization.

To construct a low variance set, and hence provide a suitable description of the moored WEC device to the system identification procedure, the average ETFE can be straightforwardly computed:

$$\bar{H}(j\omega) = \frac{1}{N_j} \sum_{j=1}^{N_j} H_j(j\omega). \tag{9}$$

Remark 4. Note that, in contrast to $H_0(j\omega)$ in Eq. (6), the average ETFE $\bar{H}(j\omega)$ in (9) effectively includes information of the mooring dynamics, via virtue of the proposed I/O characterization procedure, aided by the use of a high-fidelity mooring solver OF to compute the corresponding I/O set.

With the definition of the average ETFE in (9), standard frequency-domain system identification procedures can be directly considered (see *e.g.* [27]), to compute a parametric model of the moored WEC device for optimal control purposes. In particular, such a procedure delivers a representative state-space model of the WEC system

$$\Sigma : \begin{cases} \dot{x}(t) = Ax(t) + B\xi(t), \\ v(t) = C_v x(t), \\ z(t) = C_z x(t), \end{cases} \tag{10}$$

including the corresponding mooring influence within the I/O device dynamics. The state-vector in (10) is such that $\xi(t) \in \mathbb{R}^n$, while the associated matrices have dimensions $A \in \mathbb{R}^{n \times n}$, $\{B, C_v^\mathsf{T}, C_z^\mathsf{T}\} \subset \mathbb{R}^n$, where n denotes the order (dimension) of the identified model. Note that, as included within (10), the device position (which is simply $z = \int v$) can be also obtained straightforwardly, by inclusion of an additional output matrix accordingly.

Given that the optimal control procedure, adopted within Section 4 of this paper, is based upon a discrete-time representation of the moored WEC model, a standard zero-order-hold procedure (see *e.g.* [29]) can be applied to Σ in (10), resulting in a equivalent discrete-time state-space representation

$$\Sigma_d : \begin{cases} x_d(k+1) = A_d x_d(k) + B_d \xi_d(k), \\ \dot{z}(k) = C_{dv} x_d(k), \\ z(k) = C_{dz} x_d(k), \end{cases} \tag{11}$$

where $k = t/T_s \in \mathbb{R}$ is the discrete-time instant, with $T_s \in \mathbb{R}^+$ the sampling time.

To illustrate the results obtained via the proposed data-based modeling procedure, Fig. 2 shows the frequency-response map which characterizes the moored WEC system, identified from the average ETFE in (9), and that associated with the original linear model, *i.e.* that corresponding with the BEM solver output, as computed in Eq. (6). To compute the former, 10 multisine signals (*i.e.* $N_j = 10$) with a set of input amplitudes $\{\gamma_j\}_{j=1}^{10}$ (see (7)) equally spaced between 20 [kN] and 250 [kN], are employed to compute the associated average ETFE (9), while the frequency set in (7) is composed of 736 elements, uniformly distributed from 0.6 [rad/s] to 6 [rad/s]. An example multisine signal, with $\gamma_j = 20$ [kN], is reported in Fig. 3, including both a time- (top) and frequency-domain (bottom) representation.

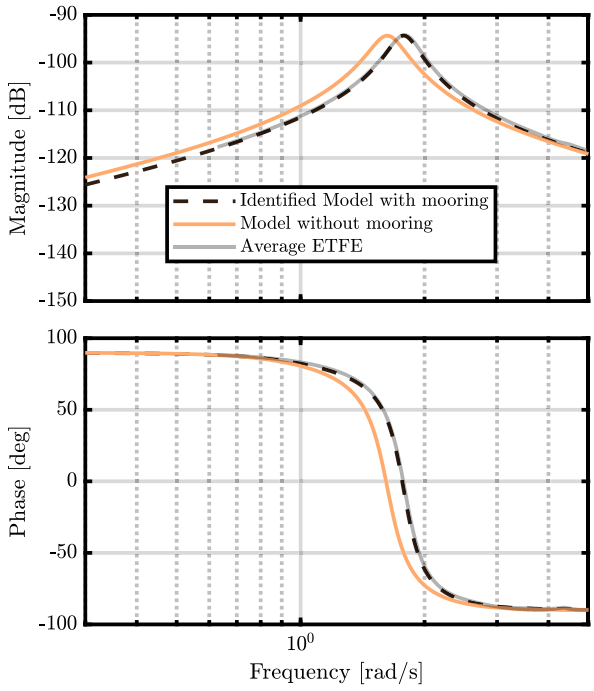

Fig. 2. Bode diagram of the model computed via the proposed mooring-informed modeling procedure (dashed-black), *i.e.* the dynamic model obtained by leveraging the average ETFE (9) (solid-gray), and that without considering the mooring system (yellow).

Remark 5. From Fig. 2, the reader can observe that the identified system dynamics for the moored WEC device fit significantly well the target average ETFE computed from the high-fidelity OrcaFlex-based response, which suggests that the mooring system has a predominantly linear response in the range excited within the identification stage. As such, in principle, the overall mooring effect could also be modeled by 'adjusting' the state-space representation in (10) with properly designed matrix corrections, *i.e.* following a grey-box modeling approach with a parametric representation composed of additional stiffness/damping/mass terms to represent the mooring system. Notwithstanding, and aiming to proposed procedure applicable to a large class of WEC devices and associated mooring systems/configurations, which might not be well-represented by a grey-box modeling approach, the (black-box) method outlined within this paper does not assume any parametric structure a-priori, being able to reflect mooring effects accurately by a suitable definition of input/output tests to excite the device in a given range of operating conditions, in a much more generic fashion, providing a best linear representation of the moored WEC. Furthermore, given the non-parametric nature of the proposed approach, other relevant nonlinear effects can be effectively included if required, by modifying the high-fidelity model accordingly (see the discussion provided in Remark 2).

From Fig. 2, it is possible to note that the resonance peak characterizing the moored WEC system differs with respect to that of the free-floating device. This 'shift' is due to the effect of the mooring system on the overall system response, stressing the fact that free-floating WEC models fails to represent the dynamics of a realistically moored device. Additionally, receding-horizon predictive strategies, such as MPC for WEC devices (see Section 4), are particularly sensitive to phase shift behaviors between the control-oriented model, and the actual WEC system [30]. This large sensitivity stems from the fact that, fundamentally, the MPC strategy aims at synchronizing wave excitation force and device velocity, thus a significant shift in the control-oriented model can lead to sub-optimal control solutions for the energy-maximizing problem.

4. Energy-maximizing control architecture

State-of-the-art WEC control algorithms aim at maximizing power extraction while respecting a given set of physical constraints (such as hull positions, velocities, and force/torque magnitudes) [31]. Among these strategies, MPC [6] has gained importance throughout the years, thanks to its inherent ability to optimize a given objective function while respecting explicit boundary sets for the problem. In the case of WEC control, the objective function is, effectively, absorbed wave power, while any constraints are given by technological (physical) limitations.

Nevertheless, as discussed within Section 1, the vast majority of wave energy MPC strategies are based on device models which neglect mooring systems. In general, WEC anchors have a negative effect in the overall energy extraction performance [14], and not including these within performance assessment can lead to misleading productivity results. Additionally, if the control model is not representative of the real moored system (*i.e.* the mooring system is neglected), the optimal condition can significantly change and the optimality associated with the control solution can be compromised, as demonstrated explicitly within Section 5.

To lay the foundations for a comparative study between state-of-the-art WEC MPC, and the proposed control-oriented mooring inclusion approach, within this section, the elements employed for the implementation of the adopted control strategy are described in detail. This comprises a detailed definition of the optimization process (cost function and problem formulation), and wave excitation force estimator with associated predictor.

Remark 6. The latter two components, *i.e.* wave excitation force and predictor, are necessary to implement a full MPC control strategy for wave energy converters, since f_w is, effectively, a non-measurable quantity (see *e.g.* [32] and the discussion provided in Section 1).

4.1. Cost function and optimization formulation

Defining the instantaneous WEC power $P : \mathbb{R}^+ \to \mathbb{R}$ as

$$P(t) = u(t)v(t), \tag{12}$$

the objective function to be minimized, within standard receding-horizon WEC control, becomes

$$J(u) = \frac{1}{T_{end}} \int_0^{T_{end}} \left(P(t) + ru(t)^2 + qz(t)^2 \right) \mathrm{d}t, \tag{13}$$

with $\{T_{end}, r, q\} \subset \mathbb{R}^+$, where T_{end} represents the length of the receding-window (see *e.g.* [6]). The terms $ru(t)^2$ and $qz(t)^2$ are employed to (soft) penalize the control action and the vertical displacement, respectively. The r term, as it is more accurately specified within Remark 7, is also necessary to guarantee objective function convexity.

For what concerns physical constraints, we assume the actuator system has limitations on the control action magnitude and a maximum admissible value for vertical buoy displacement (in order not to exceed the actuator stroke in heave). Such constraints can be traduced into two absolute value conditions, *i.e.*

$$|z(t)| < z_{max}, \quad |u(t)| < u_{max}, \quad \forall t \in [0, T_{end}], \tag{14}$$

with $\{z_{max}, u_{max}\} \subset \mathbb{R}^+$. Additionally, we note that Eq. (13) can be formulated in discrete-time domain as

$$J_d(u) = \frac{1}{N} \sum_{k=0}^{N} z(k)u(k) + r^2u(k) + qz^2(k), \tag{15}$$

where $N = \mathrm{ceil}(T_{end}/T_s) \in \mathbb{N}$.

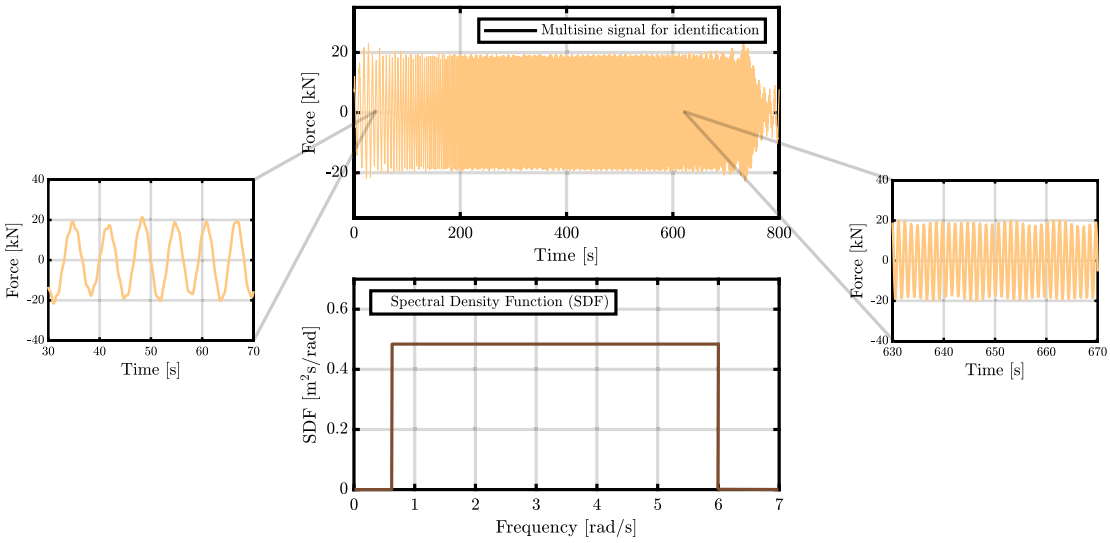

Fig. 3. Time-trace of one of the multisine signals used for the proposed data-based modeling procedure, and its associated frequency spectrum.

Given the objective function in (15), and the discrete-time equivalent of the set of defined constraints in Eq. (14), the WEC MPC optimization problem can be formulated as

$$\begin{aligned} &\min_{u} \quad J_d(u), \\ &\text{subject to:} \\ &\text{WEC dynamics in (11)}, \\ &|z(k)| < z_{max}, \\ &|u(k)| < u_{max}, \quad \forall k \in [0, N] \subset \mathbb{N}. \end{aligned} \tag{16}$$

Problem (16) can be also written in a standard quadratic programming (QP) form, which can be solved using fast, commercially available, solvers (see *e.g.* [33]). To write the optimization problem in such a QP form, it is convenient to define some auxiliary structures.

In particular, let us define the so-called α-step matrix $\mathfrak{R}_\alpha \in \mathbb{R}^\alpha$, $\alpha \in \mathbb{N}$, as

$$\mathfrak{R}_\alpha = \begin{bmatrix} C_{dv}B_d & C_{dv}A_dB_d & \dots & C_{dv}A_d^{\alpha-1}B_d \end{bmatrix}^\mathsf{T}, \tag{17}$$

and let the β-step observability matrix $\mathfrak{O}_\beta \in \mathbb{R}^{\beta \times n}$, $\beta \in \mathbb{N}$, be

$$\mathfrak{O}_\beta = \begin{bmatrix} C_{dv} & C_{dv}A_d & \dots & C_{dv}A_d^{\beta-1} \end{bmatrix}^\mathsf{T}. \tag{18}$$

Furthermore, we define the matrices $\Psi \in \mathbb{R}^{N+1 \times N+1}$, $\Upsilon \in \mathbb{R}^{N+1 \times N}$ and $\Delta \in \mathbb{R}^{N+1}$ as

$$\begin{aligned} \Psi &= \begin{bmatrix} 0 & 0 & 0 & \ddots & 0 & 0 \\ \mathfrak{R}_N & \mathfrak{R}_{N-1} & \mathfrak{R}_{N-2} & \dots & \mathfrak{R}_1 & 0 \end{bmatrix}, \\ \Upsilon &= \begin{bmatrix} 0 & 0 & 0 & \ddots & 0 \\ \mathfrak{R}_N & \mathfrak{R}_{N-1} & \mathfrak{R}_{N-2} & \dots & \mathfrak{R}_1 \end{bmatrix}, \\ \Delta &= \mathfrak{O}_{N+1}. \end{aligned} \tag{19}$$

In addition, we note that, substituting the output matrix C_{dv} with C_{dz}, one can define Ψ_{pos}, Υ_{pos}, and Δ_{pos}, analogously to (19) for the case of device displacement z.

Defining $R = r\mathbb{I}_{N+1}$ and $Q = q\mathbb{I}_{N+1}$, the standard QP form for problem (16) is:

$$\begin{aligned} &U_{0\,opt}^N = \arg\min_{U_0^N} \frac{1}{2}(U_0^N)^\mathsf{T}\mathcal{H}U_0^N + \mathcal{F}^\mathsf{T}U_0^N, \\ &\text{subject to:} \\ &A_{con}U_0^N \leq b, \end{aligned} \tag{20}$$

where

$$\begin{aligned} \mathcal{H} &= \Psi + \Psi^T + 2R + 2\Psi_{pos}^\mathsf{T}Q\Psi_{pos}, \\ \mathcal{F} &= (\Delta + 2\Psi_{pos}^\mathsf{T}Q\Delta_{pos})x_d(k) + (\Upsilon + 2\Psi_{pos}^\mathsf{T}Q\Upsilon_{pos})F_{w0}^{N-1}, \\ A_{con} &= \begin{bmatrix} \mathbb{I}_{N+1} \\ -\mathbb{I}_{N+1} \\ \Psi_{pos} \\ -\Psi_{pos} \end{bmatrix}, \\ b &= \begin{bmatrix} U_{max} \\ U_{max} \\ Z_{max} - \Delta_{pos}x(k) - \Upsilon_{pos}F_{w0}^{N-1} \\ Z_{max} + \Delta_{pos}x(k) + \Upsilon_{pos}F_{w0}^{N-1} \end{bmatrix}, \\ Z_{max} &= \mathbf{1}_{N+1}z_{max}, \\ U_{max} &= \mathbf{1}_{N+1}u_{max}. \end{aligned} \tag{21}$$

Remark 7. The power term $P(t)$ in (12) introduces a non-convex behavior in the cost function (13), as highlighted in [6]. This, in turn, compromises the well-posedness of the associated QP problem. To avoid such a scenario, a proper choice of the weights q and r can restore the positive-definiteness of the Hessian matrix associated with $\mathcal{H}$ (*i.e.* the cost function convexity), and hence regularize the problem (20) [6].

4.2. Wave force prediction

One of the most critical aspects within MPC applications in wave energy is related with the wave excitation force signal. In fact, the solution of problem (20) strongly depends on the future wave excitation

force signal affecting the moored WEC system. Nevertheless, in practice, an exact forecast of such force is never available, thus inducing a non-causal behavior in (20) (see *e.g.* [9]).

To circumvent this issue, forecasting strategies are employed to predict the wave excitation force signal over the prediction horizon N. Such predictors should ideally be computationally cheap, so as to avoid compromising the real-time loop implementation. Furthermore, these forecasting strategies must be internally stable, so as to guarantee provision of bounded wave excitation force estimates.

Among state-of-the-art strategies [10], auto regressive (AR) models have proven to be effective in accurately forecasting the short-time behavior of ocean waves. An AR model defines, at a given discrete instant k, the future value of the considered wave excitation force signal as a linear combination of its previous measurements, *i.e.*

$$\hat{f}_w(k+1) = \sum_{i=0}^{h} a_i f_w(k-i) + \varepsilon(i), \tag{22}$$

where $h \in \mathbb{N}$ is the model order, $a_i \in \mathbb{R}$ is the ith coefficient of the model parameter vector $\boldsymbol{a} \in \mathbb{R}^h$, and $\varepsilon(i) \in \mathbb{R}^+$ is a white noise signal.

Remark 8. The wave surface elevation, and hence the associated wave excitation force, is a stochastic process whose distribution changes over time [34]. Consequently, assuming that the moored WEC operates in a large set of conditions, a forecasting strategy has to change the corresponding wave model for every particular sea state, to effectively deliver accurate wave excitation forecasting values. Within this viewpoint, training the AR model on a pre-defined data set may result inaccurate, since wave conditions, which differ from the spectral representation of the training set, may be imprecisely modeled.

Following the discussion provided in Remark 8, and to cope with the non-stationary nature of the wave process, a recursive least squares filter (RLS) [35] is employed within this study, to estimate, at each time-step, the AR model parameters $\boldsymbol{a}$. In particular, let the excitation force m past values, evaluated at time k, be

$$f_w^{k-m|k} = \begin{bmatrix} f_w(k) & f_w(k-1) & \dots & f_w(k-m+1) \end{bmatrix}^\mathsf{T} \tag{23}$$

with $f_w^{k-m|k} \in \mathbb{R}^m$ and $m \in \mathbb{N}$. To estimate the AR model parameters, an approach similar to [36] is adopted, where $\boldsymbol{a}^k \in \mathbb{R}^h$ is the set of parameters employed for prediction at time step k, $\lambda \in \mathbb{R}$ is the so-called forgetting factor, and $\mathcal{A}^k \in \mathbb{R}^{h\times h}$ is the set of past estimated model parameters, defined as

$$\mathcal{A}^k = \begin{bmatrix} \boldsymbol{a}^k & \boldsymbol{a}^{k-1} & \dots & \boldsymbol{a}^{k-h+1} \end{bmatrix}. \tag{24}$$

Algorithm 1 describes the RLS filter employed to retrieve the AR model parameters, while Algorithm 2 is the prediction computation in itself.

Algorithm 1 Recursive Least Squares

Initialization:
$\mathcal{A}^{h-1} = 0$;
while $k \geq h$ **do**
$e(k) = f_w(k) - \boldsymbol{a}^{k-1} f_w^{k-h-1|k-1}$;
$r(k) = \lambda^{-1}\mathcal{A}^{k-1} f_w^{k-h-1|k-1}$;
$K(k) = r(k)/(f_w^{k-h-1|k-1})^\mathsf{T} r(k) + 1)$;
$\boldsymbol{a}^k = \boldsymbol{a}^{k-1} + K(k)e(k)$;
$\mathcal{A}^k = \lambda^{-1}\mathcal{A}^{k-1} - K(k)r(k)^\mathsf{T}$;
$k = k + 1$;
end while
Compute the prediction $\hat{f}_w^{k+1|k+p}$ with Algorithm 2.

The tuning parameters, for the process described immediately above, are the forgetting factor λ and the model order h. The main objective consists in minimizing the one-step prediction error between the real excitation force and the forecast. To do that, the selected strategy is the following: Start with a plausible parameter for static AR models (see *e.g.* [10]) and perform exhaustive parametric simulations (varying λ) with a set of wave signals. Once λ is fixed, the same procedure is repeated varying h. Note that, it is important to avoid choosing an excessively high order for the AR model, so as not to compromise the real-time performance of the overall algorithm.

Algorithm 2 Iterative prediction routine

for j = 1:N **do**
$\hat{f}_w(k+j) = \sum_{i=1}^{h} a_i f_w(k+j-i) + \varepsilon(i)$;
$f_w(k+j) = \hat{f}_w(k+j)$.
end for

Remark 9. A necessary condition for the optimal control problem requires the wave forecast to be bounded. However, it is often difficult to constrain the RLS filter to provide a set of stable AR coefficients. To cope with this issue, a white noise signal is included inside as part of the set of wave excitation force data, according with the necessary energy to ensure the required stability condition (see *e.g.* [37]).

4.3. Wave force estimation

The predictor adopted within this study, described in Section 4.2, relies on the availability of measurements of the wave force f_w exciting the moored WEC. Nevertheless, as it is well-known in the field, such possibility is hindered by the physical limit to implement pressure probes on the hull of a moving system [38]. A common alternative resides in providing the predictor with an *estimate* of the wave excitation force. Among state-of-the-art strategies [32], a steady-state Kalman-Bucy filter, as in [39], is adopted within this study, as described in the following.

Recalling Eq. (10), it is possible to approximately model the wave excitation force as a harmonic oscillator. The correspondent autonomous dynamical system is

$$\Sigma_w : \begin{cases} \dot{\kappa}(t) = S\kappa(t), \\ f_w(t) = E\kappa(t), \end{cases} \tag{25}$$

with

$$S = \bigoplus_{i=1}^{n_\omega} \begin{bmatrix} 0 & \omega_i^o \\ -\omega_i^o & 0 \end{bmatrix}, \qquad E = k_{ho}\mathbf{1}_{2n_\omega}^\mathsf{T}, \tag{26}$$

where $n_\omega \in \mathbb{N}$ is the number of selected frequency components, $\mathcal{F} = \{\omega_i^o\}_{i=1}^{N_\omega} \subset \mathbb{R}$ their corresponding set, $S \in \mathbb{R}^{2n_\omega\times 2n_\omega}$ and $k_{ho} \in \mathbb{R}/0$.

Using the representation in (25), it is possible to write an associated 'augmented' model:

$$\begin{cases} \dot{x}_{aug}(t) = A_{aug}x_{aug}(t) + B_{aug}u(t), \\ \dot{z}(t) = C_{aug}x_{aug}(t), \\ f_w(t) = C_w x_{aug}(t), \end{cases} \tag{27}$$

with $x_{aug}(t) = [x(t)^\mathsf{T}\ \kappa(t)^\mathsf{T}]^\mathsf{T} \in \mathbb{R}^{n+2n_\omega}$, and where

$$A_{aug} = \begin{bmatrix} A & BE \\ 0 & S \end{bmatrix}, \qquad C_w = \begin{bmatrix} 0 & E \end{bmatrix}, \qquad B_{aug} = \begin{bmatrix} B \\ 0 \end{bmatrix}, \qquad C_{aug} = \begin{bmatrix} C_v & 0 \end{bmatrix}. \tag{28}$$

Since the pair (A_{aug}, C_{aug}) is guaranteed to be observable, it is possible to design a full-state observer

$$\dot{\bar{x}}_{aug}(t) = A_{aug}\bar{x}_{aug}(t) + B_{aug}u(t) + L(v(t) - C_{aug}\bar{x}_{aug}(t)), \tag{29}$$

where the superscript $\{\bar{\cdot}\}$ stands for the signal estimate, and $L \in \mathbb{R}^{n+2n_\omega}$ is a static feedback gain such that

$$\lim_{t\to\infty} \|\bar{x}_{aug}(t) - x_{aug}(t)\| = 0. \tag{30}$$

Such gain L can be computed in terms of the solution of the following [40] set of equations:

$$\begin{aligned} &A_{aug}^{\mathsf{T}} P_o - P B_{aug} R_o^{-1} B_{aug}^{\mathsf{T}} P_o + Q_o = 0, \\ &L = R_o^{-1} B_{aug}^{\mathsf{T}} P_o, \end{aligned} \tag{31}$$

with $P_o \in \mathbb{R}^{n+2n_\omega \times n+2n_\omega}$, $Q_o = q_{obs}\mathbb{I}_{n+2n_\omega}$, $R_o = r_{obs}$, and $\{q_{obs}, r_{obs}\} \subset \mathbb{R}$.

Remark 10. Though a simplified expression for the observer is presented in Eq. (27), for notation convenience, we note that the matrices Q_o and R_o are related to process and measurement noise affecting the moored WEC, respectively. As it is customary in the control/estimation literature, Q_o and R_o are regarded as design parameters, used to modify the internal dynamics of the observer via the computation of L in (31).

In addition, as stressed in [39], the choice of n_ω is a critical parameter: the inclusion of non-representative frequencies, or the omission of some fundamental components, can lead to poor estimation results. If the estimator does not accurately describe the wave excitation signal, the control algorithm solution does not satisfy optimal conditions. Nevertheless, the use of an excessive number of harmonics may result demanding for the device hardware, compromising the algorithm real-time feasibility, so that a reasonable balance should be achieved at the design/synthesis stage.

Remark 11. Since the optimization problem (20) requires the state information $x(k)$, the wave force estimator is also employed to obtain a state estimate $\bar{x}(k)$. Such quantity can be retrieved straightforwardly, given that the observer provides an estimate of the augmented state, namely $\bar{x}_{aug}(k)$.

5. Results

This section presents a detailed account of the main results of the paper, providing a thorough evaluation of the performance associated with the optimal WEC controller, described within Section 4, for different simulation scenarios. We note that, for the totality of the simulation cases, the dynamics associated with the WEC system are always resolved[1] via the high-fidelity model in OF, as described within Section 2.1. The simulation environment considers a 3-DoF scenario, in which the device is free to move on in heave, surge, and pitch DoFs. In particular, and in reference to Fig. 1, the WEC is allowed to translate on the $x-$ and $z-$axes, and to rotate around the $x-z$-plane orthogonal axis. Note that the term 'high-fidelity' is used, within this paper, to refer to a dynamical representation able to include an accurate account of mooring effects on the WEC system (which are the core topic of this study) via a dynamic lumped-mass solver (OrcaFlex).

In particular, to evaluate the performance of the proposed MPC strategy, three different assessment configurations are considered:

(S-1) *Ideal scenario*: In this evaluation case, the high-fidelity OF simulation model *does not* include the mooring dynamics, *i.e.* the device is free to move without mooring action. Furthermore, the MPC strategy is based on the unmoored model accordingly, as computed in Section 2. This case is ideal (unrealistic), in the sense that: a) the WEC does not feature a mooring system (and hence performance tends to be overestimated - see [14]), and (b) the controller uses an exact description of the BEM model employed by OrcaFlex, *i.e.* it incorporates an exact description of the (unmoored) WEC dynamics.

[1] Simulations are carried out a on target PC with AMD Ryzen 9 3900X 12-Core, 3.79 [GHz] Processor.

Table 2
Chracteristics associated with the considered wave sea states.

Waves		
ID	T_e [s]	H_s [m]
W_1	6.4	2.1
W_2	4.6	1.5
W_3	3.9	0.9
W_4	3.4	0.9

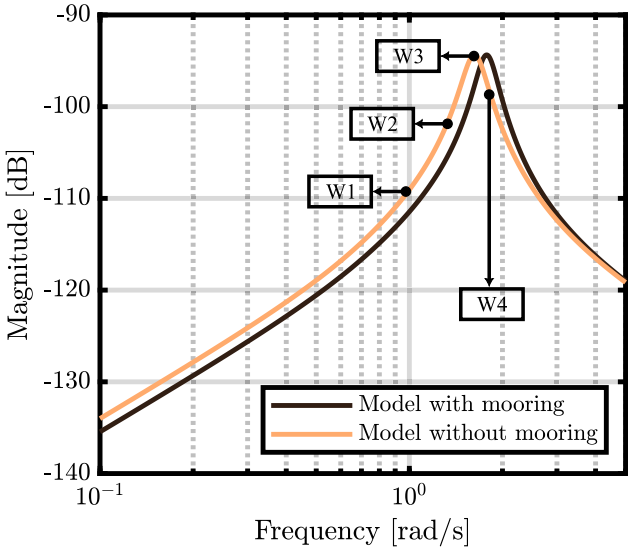

Fig. 4. Location each tested sea state with respect to their energetic periods (pins), with respect to unmoored and (identified) moored device dynamics.

(S-2) *Nominal scenario*: In this case, the high-fidelity OF simulation model *does* include the mooring dynamics, but the control architecture is based on a model of the unmoored dynamics. This case is hence termed 'nominal', since this would be the exact scenario if one would attempt to apply/replicate the vast majority of the WEC controllers (and associated performances) available within the literature, to a moored WEC device.

(S-3) *Proposed scenario*: This case evaluates the overall strategy proposed within this study, *i.e.* the high-fidelity OF simulation model *does* include the mooring dynamics, and the control architecture employs the representative data-based model computed as in Section 3.

As input for all the scenarios described above, four different wave characterizations are chosen, with parameters are reported in Table 2, where each stochastic description is defined in terms of a JONSWAP spectrum (see [41]), with a fixed peak-enhancement factor of 3.3. The wave parameters in Table 2 are adopted from the Pantelleria site scatter data set [42], representing a realistic set of operating conditions. We further note that the choice of waves is performed to excite the system in different operating conditions, so as to provide representative performance results for a moored WEC. In particular, Fig. 4 shows the frequency associated with each defined energetic period, alongside the frequency response map for both the unmoored (BEM), and representative (as computed in Section 3) moored WEC models.

5.1. Model validation

Both to quantify the underlying mooring effects present on the case study, and validate the modeling strategy proposed in Section 3, we

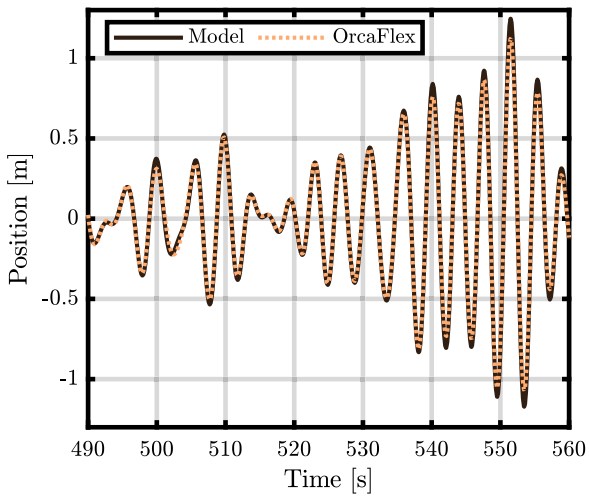

Fig. 5. Time-domain displacement both for the high-fidelity OF model (yellow), and the data-based model in (11) (black).

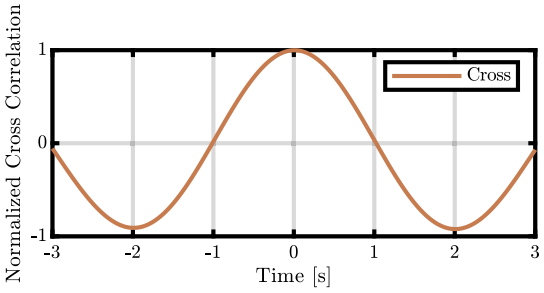

Fig. 6. Normlized cross-correlation between displacement as computed via the high-fidelity OF model and the data-based model in (11).

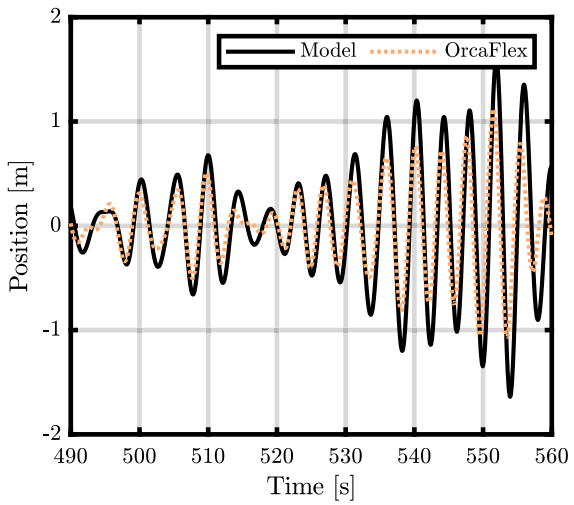

Fig. 7. Time-domain displacement both for the high-fidelity OF model (yellow), and the model computed following Section 2.3 (black), which does not feature a mooring representation.

Table 3
Control system tuning parameters.

Control Parameters	
T_s	0.1 [s]
N	100
u_{max}	$1 \cdot 10^6$ [N]
z_{max}	1 [m]
r	$4 \cdot 10^{-7}$
q_{pos}	$1 \cdot 10^{-5}$
$\mathcal{F}$	{0.98, 1.36, 1.61, 1.84} [rad/s]
k_{ho}	$1 \cdot 10^8$
q_{obs}	$1 \cdot 10^2$
r_{obs}	0.1
h	100
λ	10^{-3}

briefly present, in this section, a performance analysis of the identified model, also including a comparison with the standard modeling approach considered within the literature, *i.e.* without considering mooring dynamics (as in Section 2.3).

To achieve this, the identified system (11) response has been compared with that produced by the high-fidelity model (in OF), which effectively includes a full account of the nonlinear dynamics associated with the anchored device. To provide a fair validation/comparison, the two systems are excited with the same wave elevation input signal, corresponding to W_2 in Table 2.

Such tests demonstrates that system (11) effectively represent the heaving point absorber motion response, showing good responses both in terms of lag conditions, as it can be seen from the cross correlation function of the two signals in Fig. 6, and in terms of the signal matching, which can be observed in Fig. 5. For the sake of completeness, Fig. 7 comprises the same validation test, under identical conditions, carried out with a system model which does not feature a mooring representation. As expected, a discrepancy between the two motions arise in the results, illustrating the effects that neglecting mooring forces can have on the system representation.

5.2. Control performance

To provide a fair comparison, the control parameters are kept constant throughout all the scenarios. The values for r and q_{pos} are chosen to guarantee convexity of the associated QP form while weighting sufficiently the power term in the cost function (see Remark 7). The elements of the set $\mathcal{F}$ (see Section 4.3) are chosen in terms of the combination of all the sea state energetic periods T_e (as listed in Table 2). The observer and AR model order parameters are chosen in simulation, to guarantee satisfactory performance in terms of wave (and state) estimation and excitation force prediction. Such tuning choices are reported in Table 3.

Remark 12. As per the sign convention adopted from the early beginning of this paper, *i.e.* Eq. (2), a negative value in power absorption (and consequently energy) indicates that energy is effectively being extracted from waves.

In Fig. 8, the difference in terms of energy production under the three different scenarios can be clearly appreciated. The ideal setup (S-1) proves to be the most power-productive configuration. As previously discussed within this section, this result can be easily justified by the fact that: (a) the unmoored system has inherent capabilities to absorb more mechanical energy from the wave resource (since it is effectively free to move), and (b) the model used to synthesize the controller coincides with that emulated by the OF solver in unmoored conditions. Nevertheless, such scenario cannot be considered as a benchmark to evaluate the other two strategies, since it does not represent a realistic operating condition. As a matter of fact, the results associated with (S-1) are intended to assess the impact that anchoring the device has on the total productivity (and constraint handling) with an ideal controller (*i.e.* with exact knowledge of the unmoored system dynamics) . For what concerns the moored WEC device, *i.e.* in realistic conditions,

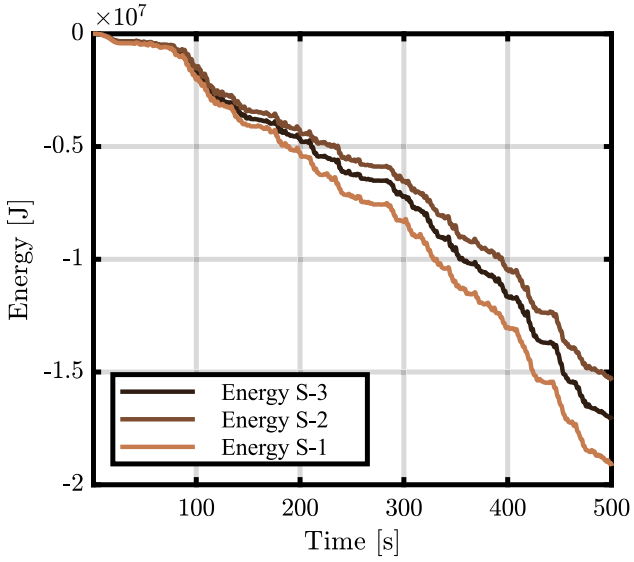

Fig. 8. Energy production for W_1.

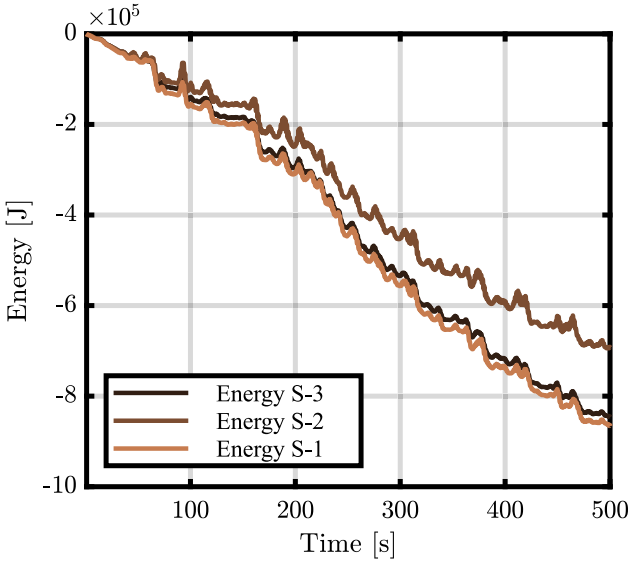

Fig. 10. Energy production for W_3.

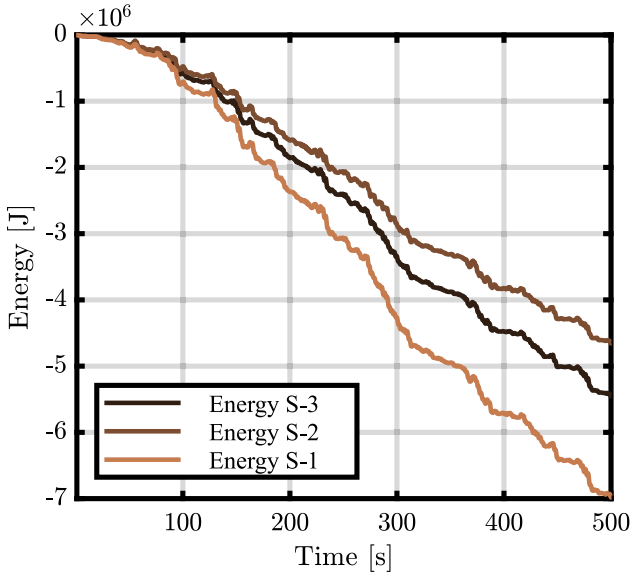

Fig. 9. Energy production for W_2.

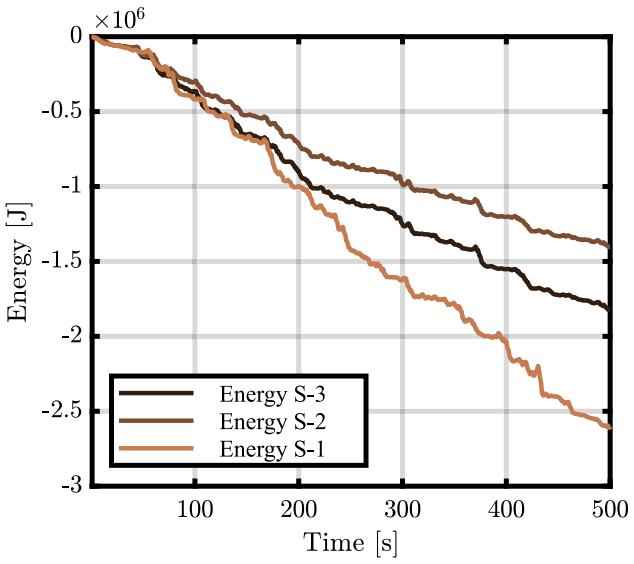

Fig. 11. Energy production for W_4.

the proposed control strategy shows higher productivity results than the nominal configuration. This demonstrates that a inclusion of the mooring dynamics within the control synthesis procedure, via the representative modeling technique proposed in Section 3 of this paper, represents more accurately the real process, and hence the final control performance is enhanced with such fundamental information. For the sake of completeness, the energy extraction results for the remaining sea states are reported in Figs. 9, 10, and 11, respectively. Note that, as can be appreciated from Fig. 10, S-1 and S-3 configurations show similar productivity results for W_3. In particular, as it can be seen in Fig. 4, the peak period (alternatively peak frequency) associated with W_3 lies precisely on the resonance peak of the unmoored system. The corresponding identified model for the moored WEC, which has been proved to be effective in describing the associated motion (see the validation results in Section 5.1), has a similar behavior in the neighborhood of the unmoored resonance peak. This implies that, under the discussed scenario, the productivity of the device featuring the mooring system is similar to the 'free-floating' system, reason for which the energy production linked to S-1 and S-3 are similar in the case of W_3.

In parallel, the MPC strategy is expected to keep the imposed constraints on the vertical displacement z and the control action magnitude u. Fig. 12 demonstrates that the controller solution, as computed in the totality of the evaluated scenarios, is consistently able to manage the position constraint, independently from its energy-maximizing performance. Same applies for the control limitations, which are equally respected in all the scenarios, as per Fig. 13.

5.3. Estimation and prediction performance

An additional key aspect regards the wave estimate quality, which naturally affects the performance of the synthesized MPC solution. Fig. 14 shows the wave force estimation performance for the three different scenarios, for sea state W_4 and W_1. As expected, the S-1 strategy estimates adequately the wave excitation force signal in both the simulation cases, while the nominal (S-2) does not properly track the actual excitation force, since the model defined in the observer

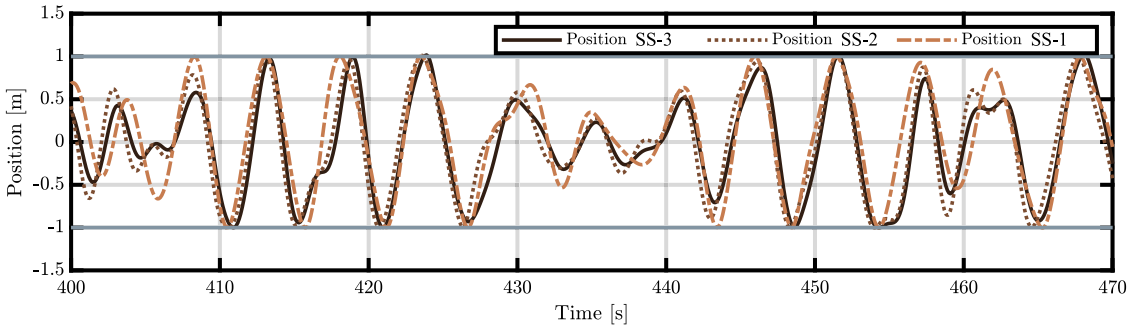

Fig. 12. Point absorber vertical position for (S-1), (S-2) and (S-3). Simulation referred to W_1.

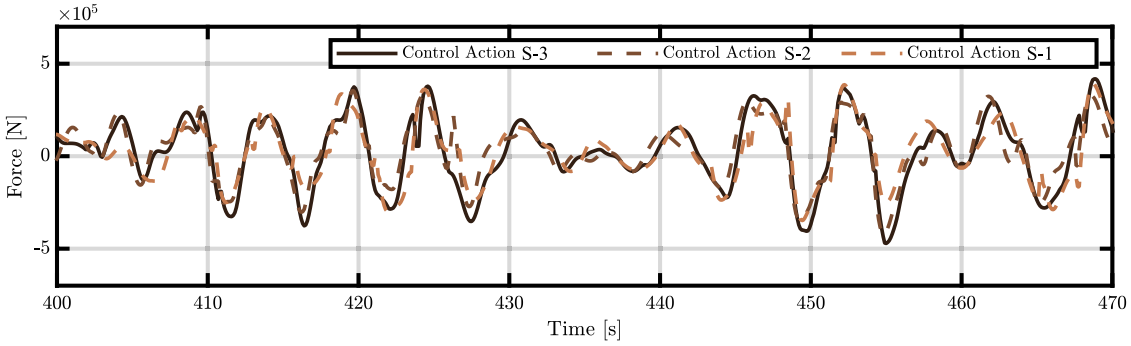

Fig. 13. Applied control action for (S-3) (dark brown), (S-2) (light dashed brown), and (S-1) (dashed yellow). Results referred to SS_1.

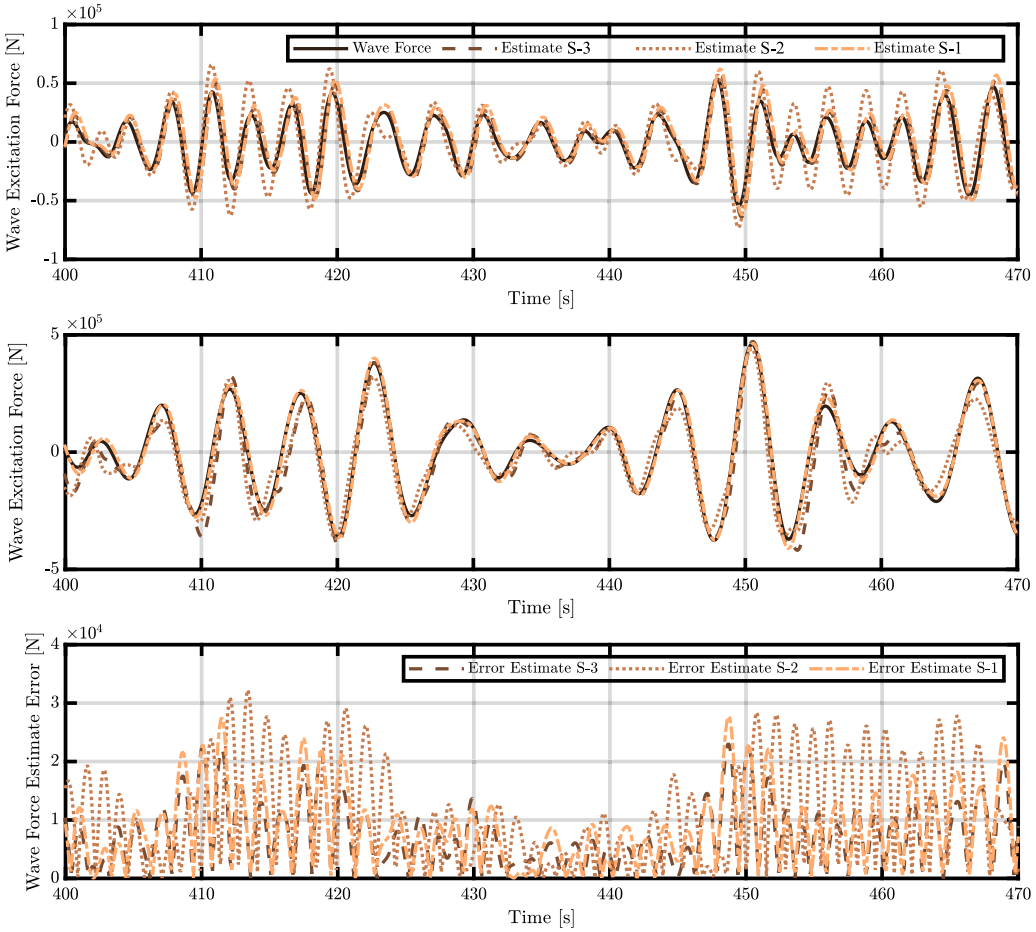

Fig. 14. Wave excitation force estimation: real (target) excitation force (dark brown), (S-3) (dashed brown), (S-2) (light dashed brown) and (S-1) (dashed yellow) strategy. The upper figure refers to W_4, while the middle plot illustrates estimation performance for W_1.The lower plot is the estimation error absolute value of S-3, S-2 and S-1, related to the results in W_4 (upper plot).

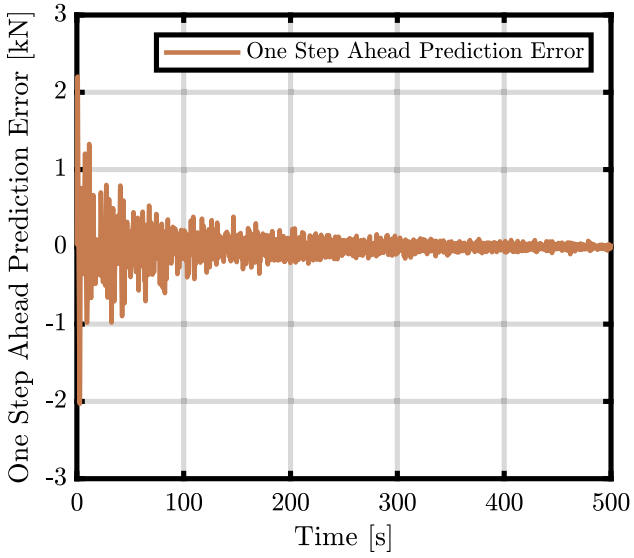

Fig. 15. One step ahead prediction error for the RLS procedure. Results related to (S-3) in W_1 sea conditions.

does not describe effectively the real system. As highlighted in problem (20), the solution explicitly depends on the current (and future) value of the wave excitation. If such signal is not estimated precisely, the obtained MPC solution is, naturally, distant from the optimal control action. In contrast, the other two estimators (*i.e.* those synthesized according to S-2 and S-3) manage to represent more accurately the real device dynamics, thus providing better wave excitation force estimates at every control step.

For what concerns the future value of the wave excitation force provided to the solver, an example of the performance of the proposed RLS in (1) is given in Fig. 15. In particular, this figure reports the one-step-ahead prediction error obtained over time with the filter parameters estimate, with reference to the proposed strategy (S-3), evaluated in W-1 sea state conditions. The RLS filter converges as the simulation advances, meaning that the prediction accuracy increases over time, as expected from the RLS implementation.

Remark 13. It must be stressed that the AR model in (22) is obtained with *estimated* values of the wave excitation force. Consequently, it is reasonable to deduce that the one-step-ahead prediction error is lower for a more precise wave estimation algorithm, as in the case of S-1 or S-3, and increases when the estimation algorithm is not able to provide reliable estimates of the input wave signal, as in S-2.

6. Conclusions

Given the importance of model-based optimal control strategies in wave energy conversion systems, the paper proposes to investigate the effects of neglecting the mooring modeling stage in the control-oriented model design, with special attention to energy production performance and constraint fulfillment. The paper introduces the WEC device and its mooring system model, the practical implementation of the optimization problem for the MPC control algorithm, the auxiliary estimator, and predictor systems. Furthermore, in an effort to incorporate the mooring dynamics within optimal control synthesis, a data-based control-oriented modeling procedure is proposed, able to provide representative models for moored WEC systems.

Within performance assessment, three different scenarios are tested (S-1, S-2, and S-3). The results show that the power production in the nominal scenario (S-2) is lower in all sea states analyzed, with respect to the ideal case (S-1), despite the fact they share the same control-oriented model. To reduce the gap between ideal and nominal scenarios, passing through the proposed mooring-informed modeling stage shows to be an efficient procedure, demonstrated by the improvements on every sea state tested, in terms of energy harvesting efficiency. Furthermore, the imposed constraints on the point absorber vertical displacement and control action are consistently fulfilled, in spite of the actual energy-maximizing performance of the computed control solution.

CRediT authorship contribution statement

Guglielmo Papini: Methodology, Software, Validation, Formal analysis, Investigation, Data curation, Writing – original draft, Visualization. **Bruno Paduano:** Methodology, Software, Validation, Formal analysis, Investigation, Data curation, Writing – review & editing. **Edoardo Pasta:** Methodology, Software, Validation, Formal analysis, Investigation, Data curation, Writing – review & editing. **Fabio Carapellese:** Methodology, Software, Validation, Formal analysis, Investigation, Data curation, Writing – review & editing. **Giuliana Mattiazzo:** Resources, Supervision, Project administration, Funding acquisition. **Nicolás Faedo:** Methodology, Formal analysis, Resources, Supervision, Project administration, Funding acquisition, Writing – review & editing.

Declaration of competing interest

The authors declare that they have no known competing financial interests or personal relationships that could have appeared to influence the work reported in this paper.

Acknowledgments

N. Faedo has received funding from the European Union's Horizon 2020 research and innovation programme under the Marie Sklodowska-Curie grant agreement No 101024372. The results of this publication reflect only the author's view and the European Commission is not responsible for any use that may be made of the information it contains.

References

[1] Giuliana Mattiazzo, State of the art and perspectives of wave energy in the Mediterranean Sea: Backstage of ISWEC, Front. Energy Res. 7 (2019).
[2] Bingyong Guo, John V. Ringwood, A review of wave energy technology from a research and commercial perspective, IET Renew. Power Gener. 15 (14) (2021) 3065–3090.
[3] Bingyong Guo, John V. Ringwood, Geometric optimisation of wave energy conversion devices: A survey, Appl. Energy 297 (2021) 117100.
[4] John V. Ringwood, Giorgio Bacelli, Francesco Fusco, Energy-maximizing control of wave-energy converters: The development of control system technology to optimize their operation, IEEE Control Syst. Mag. 34 (5) (2014) 30–55.
[5] Rudy Nie, Jeff Scruggs, Allan Chertok, Darragh Clabby, Mirko Previsic, Anantha Karthikeyan, Optimal causal control of wave energy converters in stochastic waves – Accommodating nonlinear dynamic and loss models, Selected Papers from the European Wave and Tidal Energy Conference 2015, Nante, France, Int. J. Mar. Energy 15 (2016) 41–55.
[6] Guang Li, Mike R. Belmont, Model predictive control of a sea wave energy converter: a convex approach, 19th IFAC World Congress, IFAC Proc. Vol. 47 (3) (2014) 11987–11992.
[7] N. Faedo, G. Giorgi, J.V. Ringwood, G. Mattiazzo, Optimal control of wave energy systems considering nonlinear Froude–Krylov effects: control-oriented modelling and moment-based control, Nonlinear Dynam. 109 (3) (2022) 1777–1804.
[8] Fabio Carapellese, Edoardo Pasta, Bruno Paduano, Nicolás Faedo, Giuliana Mattiazzo, Intuitive LTI energy-maximising control for multi-degree of freedom wave energy converters: The PeWEC case, Ocean Eng. 256 (2022).
[9] J.T. Scruggs, S.M. Lattanzio, A.A. Taflanidis, I.L. Cassidy, Optimal causal control of a wave energy converter in a random sea, Appl. Ocean Res. 42 (2013) 1–15.
[10] Yerai Peña-Sanchez, Alexis Mérigaud, John V. Ringwood, Short-term forecasting of sea surface elevation for wave energy applications: The autoregressive model revisited, IEEE J. Ocean. Eng. 45 (2) (2020) 462–471.
[11] Nicolás Faedo, Ulises Bussi, Yerai Peña-Sanchez, Christian Windt, John V. Ringwood, A simple and effective excitation force estimator for wave energy systems, IEEE Trans. Sustain. Energy 13 (1) (2022) 241–250.

[12] WMO, Guide To Wave Analysis and Forecasting, Vol. 1998, 1998.
[13] DNV, DNV-OS-E301 Position mooring, Technical Report, 2015, URL www.dnvgl.com.
[14] Bruno Paduano, Edoardo Pasta, Guglielmo Papini, Fabio Carapellese, Giovanni Bracco, Mooring influence on the productivity of a pitching wave energy converter, in: OCEANS 2021: San Diego – Porto, 2021, pp. 1–6.
[15] Eric Gubesch, Nagi Abdussamie, Irene Penesis, Christopher Chin, Effects of mooring configurations on the hydrodynamic performance of a floating offshore oscillating water column wave energy converter, Renew. Sustain. Energy Rev. 166 (2022) 112643.
[16] B. Paduano, F. Carapellese, E. Pasta, N. Faedo, G. Mattiazzo, Optimal controller tuning for a nonlinear moored wave energy converter via non-parametric frequency-domain techniques, Trends Renew. Energies Offshore (2022) 393–400.
[17] Josh Davidson, John V. Ringwood, Mathematical modelling of mooring systems for wave energy converters—A review, Energies 10 (5) (2017) 666.
[18] Orcawave manual, 2023, https://www.orcina.com/webhelp/OrcaWave/Default.htm (accessed on: 10/01/2023).
[19] Johannes Falnes, Adi Kurniawan, Ocean Waves and Oscillating Systems: Linear Interactions Including Wave-Energy Extraction, Vol. 8, Cambridge University Press, UK, 2020.
[20] Matt Folley, Numerical Modelling of Wave Energy Converters - 1st Edition, 2016.
[21] John V. Ringwood, Siyuan Zhan, Nicolás Faedo, Empowering wave energy with control technology: Possibilities and pitfalls, Annu. Rev. Control (2023).
[22] W.E. Cummins, The Impulse Response Function and Ship Motions, Navy Department, David Taylor Model Basin, 1962.
[23] Bret Bosma, Zhe Zhang, Ted K.A. Brekken, H. Tuba Özkan-Haller, Cameron McNatt, Solomon C. Yim, Wave energy converter modeling in the frequency domain: A design guide, in: 2012 IEEE Energy Conversion Congress and Exposition (ECCE), 2012, pp. 2099–2106.
[24] Orcaflex documentation, 10.1b edition, 2020, Available online: https://www.orcina.com/releases/orcaflex-101/ (accessed on: 10/01/2023).
[25] Christian Windt, Nicolás Faedo, Markel Penalba, Frederic Dias, John V Ringwood, Reactive control of wave energy devices–the modelling paradox, Appl. Ocean Res. 109 (2021) 102574.
[26] Z. Drmač, S. Gugercin, C. Beattie, Quadrature-based vector fitting for discretized H2 approximation, SIAM J. Sci. Comput. 37 (2) (2015) A625–A652, Publisher: Society for Industrial and Applied Mathematics.
[27] Lennart Ljung, in: Ales Procházka, Jan Uhlíř, P.W.J. Rayner, N.G. Kingsbury (Eds.), System Identification, in: Applied and Numerical Harmonic Analysis, Birkhäuser, Boston, MA, ISBN: 978-1-4612-1768-8, 1998, pp. 163–173.
[28] J. Schoukens, R. Pintelon, E. van der Ouderaa, J. Renneboog, Survey of excitation signals for FFT based signal analyzers, IEEE Trans. Instrum. Meas. 37 (3) (1988) 342–352.
[29] K. Pohlmann, Principles of Digital Audio, McGraw-Hill Companies,Incorporated, 2005.
[30] Nicolás Faedo, Giuliana Mattiazzo, John V. Ringwood, Robust energy-maximising control of wave energy systems under input uncertainty, in: 2022 European Control Conference (ECC), IEEE, 2022, pp. 614–619.
[31] Jørgen Hals, Johannes Falnes, Torgeir Moan, Constrained optimal control of a heaving Buoy Wave-Energy converter, J. Offshore Mech. Arct. Eng. 133 (1) (2010).
[32] Yerai Peña-Sanchez, Christian Windt, Josh Davidson, John V. Ringwood, A critical comparison of excitation force estimators for wave-energy devices, IEEE Trans. Control Syst. Technol. 28 (6) (2020) 2263–2275, Conference Name: IEEE Transactions on Control Systems Technology.
[33] Odys QP solver - fast and robust QP solver for embedded MPC, 2022.
[34] Michel K. Ochi, Ocean Waves: the Stochastic Approach, Cambridge University Press, Cambridge, 1998.
[35] Paulo S.R. Diniz, Conventional RLS adaptive filter, in: Adaptive Filtering: Algorithms and Practical Implementation, Springer International Publishing, Cham, 2020, pp. 157–187.
[36] A. Schlögl, D. Flotzinger, G. Pfurtscheller, Adaptive autoregressive modeling used for single-trial EEG classification, Biomed. Tech. Biomed. Eng. 42 (6) (1997) 162–167.
[37] G. Papini, Y. Peña-Sanchez, E. Pasta, N. Faedo, Control-oriented wave surface elevation forecasting strategies: Experimental validation and comparison, in: The 22st IFAC World Congress, Yokohama, Japan, 2023.
[38] Yerai Peña-Sanchez, Marina Garcia-Abril, Francesco Paparella, John V. Ringwood, Estimation and forecasting of excitation force for arrays of wave energy devices, IEEE Trans. Sustain. Energy 9 (4) (2018) 1672–1680, Conference Name: IEEE Transactions on Sustainable Energy.
[39] M. Garcia-Abril, F. Paparella, J.V. Ringwood, Excitation force estimation and forecasting for wave energy applications, IFAC-PapersOnLine 50 (1) (2017) 14692–14697.
[40] Huibert Kwakernaak, Raphael Sivan, Bjor N.D. Tyreus, Linear optimal control systems, J. Dyn. Syst. Meas. Control 96 (3) (1974) 373–374.
[41] M. Ryabkova, V. Karaev, J. Guo, Yu. Titchenko, A review of wave spectrum models as applied to the problem of radar probing of the sea surface, J. Geophys. Res.: Oceans 124 (10) (2019) 7104–7134.
[42] Luca Liberti, Adriana Carillo, Gianmaria Sannino, Wave energy resource assessment in the mediterranean, the Italian perspective, Renew. Energy 50 (C) (2013) 938–949.